Molecular and functional identification of a novel photopigment in *Pecten* ciliary photoreceptors

Oscar Arenas,[1] Tomás Osorno,[1] Gerardo Malagón,[1] Camila Pulido,[1] María del Pilar Gomez,[1,3] and Enrico Nasi[2,3]

[1]Departamento de Biología and [2]Instituto de Genética, Universidad Nacional de Colombia, Bogotá, Colombia
[3]Marine Biological Laboratory, Woods Hole, MA

The two basic animal photoreceptor types, ciliary and microvillar, use different light-transduction schemes: their photopigments couple to G_t versus G_q proteins, respectively, to either mobilize cyclic nucleotides or trigger a lipid signaling cascade. A third class of photoreceptors has been described in the dual retina of some marine invertebrates; these present a ciliary morphology but operate via radically divergent mechanisms, prompting the suggestion that they comprise a novel lineage of light sensors. In one of these organisms, an uncommon putative opsin was uncovered that was proposed to signal through G_o. Orthologues subsequently emerged in diverse phyla, including mollusks, echinoderms, and chordates, but the cells in which they express have not been identified, and no studies corroborated their function as visual pigments or their suggested signaling mode. Conversely, in only one invertebrate species, *Pecten irradians*, have the ciliary photoreceptors been physiologically characterized, but their photopigment has not been identified molecularly. We used the transcriptome of *Pecten* retina to guide the cloning by polymerase chain reaction (PCR) and rapid amplification of cDNA ends (RACE) extensions of a new member of this group of putative opsins. In situ hybridization shows selective transcription in the distal retina, and specific antibodies identify a single band of the expected molecular mass in Western blots and distinctly label ciliary photoreceptors in retina sections. RNA interference knockdown resulted in a reduction in the early receptor current—the first manifestation of light transduction—and prevented the prolonged aftercurrent, which requires a large buildup of activated rhodopsin. We also obtained a full-length clone of the α-subunit of a G_o from *Pecten* retina complementary DNA and localized it by in situ hybridization to the distal photoreceptors. Small interfering RNA targeting this G_o caused a specific depression of the photocurrent. These results establish this novel putative opsin as a bona fide visual pigment that couples to G_o to convey the light signal.

Journal of General Physiology

INTRODUCTION

Two canonical classes of primary visual cells, dubbed ciliary and rhabdomeric photoreceptors, respectively, have been established on the basis of the structure of their light-sensing cellular specializations: either modified ciliary appendages, as in vertebrate rods and cones (Tokuyasu and Yamada, 1959), or infoldings of the plasma membrane in the form of actin-packed microvilli, as in arthropods (de Couet et al., 1984; Arikawa et al., 1990). More recently, sequence analysis of opsins from a wide range of organisms has shown that animal photopigments can also be grouped into distinct categories; two of them largely follow the two aforementioned morphological classes of photoreceptors and were therefore named C-opsins and R-opsins (Arendt et al., 2004). Because the former convey the light signal via a G_t and stimulate a phosphodiesterase to control cGMP levels (reviewed by Luo et al., 2008), whereas the latter activate G_q and trigger an inositol-lipids pathway (reviewed by Hardie and Raghu, 2001), these two opsin groups have also been labeled "G_t-coupled" and "G_q-coupled" (Shichida and Yamashita, 2003; Terakita, 2005).

A third class of photoreceptor cells, first described in the distal retina of marine bivalve mollusks of the Pectinidae family (scallops), have a ciliary morphology (Miller, 1958; Barber et al., 1967) and a hyperpolarizing receptor potential like that of vertebrate rods and cones (Gorman and McReynolds, 1969). However, they operate via profoundly different ionic mechanisms that involve light-triggered opening of ion channels (Gorman and McReynolds, 1978; Gomez and Nasi, 1994a); this calls for a different phototransduction cascade, prompting the suggestion that such cells comprise a separate lineage of light sensors (Gomez and Nasi, 2000). In fact, in a survey of signaling molecules in the eye of *Mizuhopecten* (a.k.a., *Patinopecten*), the giant scallop of northern Japan, the distal retina layer was found to be devoid of both conventional opsin types; instead, a novel putative photopigment was discovered and dubbed Scop2 (NCBI accession no. BAA22218). Furthermore, the only heterotrimeric G-protein that

Correspondence to Enrico Nasi: enasil@unal.edu.co
O. Arenas's present address is Dept. of Neuroscience, Northwestern University, Chicago, IL.
T. Osorno's present address is Dept. of Neurobiology, Harvard Medical School, Boston, MA.
G. Malagón's present address is Laboratoire de Physiologie Cérébrale, Université Renée Descartes, Paris, France.
C. Pulido's present address is Dept. of Biochemistry, Cornell University, Ithaca, NY.

The Rockefeller University Press
J. Gen. Physiol. 2018 Vol. 150 No. 3 401–415
https://doi.org/10.1085/jgp.201711938

colocalized with this unusual opsin was a G_o, which was proposed to mediate the light response (Kojima et al., 1997). There were no precedents for G_o participation in any phototransduction process. Indirect support for the notion that Scop2 may couple to G_o was provided by in vitro assays of chimeric bovine rhodopsin: replacement of the third intracellular loop with that of Scop2 decreased its competence to activate transducin (G_t), while enhancing its ability to stimulate G_o (Terakita et al., 2002). Orthologues of Scop2 have been subsequently identified in another mollusk (*Crassostrea gigas*, accession no. EKC29416), in a primitive chordate (*Branchiostoma belcheri*, Koyanagi et al., 2002; accession nos, AB050606 and AB050607), and in an echinoderm (*Strongylocentrotus purpuratus*, accession no. XM_011676116), indicating a rather widespread phylogenetic distribution. In spite of the accumulated molecular information, much remains to be learned about these putative novel light-sensing molecules, as the cells that natively express them have never been examined physiologically, and in most cases have not even been identified. Moreover, to date, only one of these opsins (from *Branchiostoma*) has been heterologously expressed and shown in vitro to bind 11-cis-retinal as a chromophore (Koyanagi et al., 2002), but, as yet, no functional reconstitution has been attained. Conclusive evidence that these molecules indeed form functional visual pigments is therefore still lacking, and so is experimental support to elucidate their mode of signaling.

The physiology of the light response of nonvertebrate ciliary hyperpolarizing photoreceptors has been investigated in detail in only one species, the bay scallop, *Pecten irradians* (McReynolds and Gorman, 1970a,b; Gomez and Nasi, 1994b,a, 1997a,b, 2005; del Pilar Gomez and Nasi, 1995, 2005; Nasi and del Pilar Gomez, 1999). However, its photopigment had not been molecularly identified. Pharmacological clues do implicate a G_o in *Pecten* photoresponsiveness, as was proposed for *Mizuhopecten*: the light response is susceptible to inhibition by pertussis toxin, which selectively targets G_i/G_o, and the photoconductance can be activated by mastoparan peptides, which are preferential activators of G_o (Gomez and Nasi, 2000). Direct evidence supported by molecular data, however, is still missing.

The purpose of the present work was to ascertain the molecular identity of the photopigment of *Pecten* ciliary photoreceptors and the G-protein that conveys the light signal. In addition to helping elucidate this third light-signaling pathway, there is an additional facet that makes this endeavor appealing: biophysical studies have established that the rhodopsin of *Pecten*—like those of several arthropods—is bistable and undergoes a large spectral shift with photoisomerization; this allows manipulation (and quantitative analysis) of its states (Cornwall and Gorman, 1983). The photopigment of *Pecten* ciliary visual cells could therefore be a useful biotechnological tool, a molecule capable of turning on—or off—a G-protein cascade by simply manipulating the chromatic content of a light stimulus.

MATERIALS AND METHODS

Specimens of *Pecten irradians* were obtained from the Aquatic Resources Division of the Marine Biological Laboratory (Woods Hole, MA).

Cell dissociation and recording

Retinae of *Pecten* were enzymatically and mechanically dissociated as previously described (Gomez and Nasi, 1994a). Patch pipettes fabricated from borosilicate glass were fire-polished and filled with an intracellular solution containing 100 mM KCl, 200 mM K-glutamate, 5 mM $MgCl_2$, 5 mM Na_2ATP, 20 mM NaCl, 1 mM EGTA, 300 mM sucrose, 10 mM Hepes, and 0.2 mM GTP, pH 7.3. Electrode resistance in ASW was 2–4 MΩ. An Optopatch amplifier (Cairn Research) was used to measure membrane currents. Data were digitized with an analogue–digital interface (DT9834; Data Translation), which served also to generate stimuli under the control of software developed in-house.

Light stimulation

Light flashes were generated either by a tungsten-halogen light source equipped with an electromechanical shutter (Uniblitz), as previously described (Gomez and Nasi, 1994a), or by a high-intensity 470-nm LED (Thorlabs). To visualize cells during experimental manipulations, deep red light illumination was used ($\lambda >$ 630 nm). To accurately estimate response latencies, the raw traces were corrected after measuring with a photodiode the actual opening delay of the shutter (when applicable), as well as the time shift introduced in the recorded current trace by the analogue low-pass filter. Light intensity was measured with a calibrated radiometer (UDT model 370) and converted to photon flux. For experiments that used broadband light, its intensity was converted to effective photons at 500 nm via in vivo calibration, as previously described (Gomez and Nasi, 1994b,a).

Immunochemistry

Polyclonal antibodies raised against the Scop2 orthologue of *Pecten* were generated by Biosynthesis (Lewisville, TX). To this end, a synthetic peptide (C-TRRNET RTRQGYMPRYIQD) derived from the predicted amino acid sequence was conjugated to keyhole limpet hemocyanin and used to immunize rabbits. The antiserum was affinity purified. For Western blots, retinae were homogenized (Teflon/glass) in lysis buffer (30 mM Tris HCl, 100 mM NaCl, 5 mM EDTA, 1% SDS, and 20% glycerol, pH 7.4) in the presence of protease inhibitors (0.25% Sigma protease inhibitor cocktail and 250 µM

PMSF), acetone-precipitated at −20°C for 1 h, and centrifuged for 10 min at 12,000 *g*. The pellet was air-dried, resuspended in sample buffer, and separated by SDS PAGE (8%). Proteins were then electrotransferred (Mini Trans-Blot; Bio-Rad) onto a nitrocellulose membrane, which was blocked overnight with 3% BSA. The membrane was sequentially incubated with primary antibodies (1:1,000, 3 h), washed, treated with alkaline phosphatase (AP)-conjugated anti-rabbit secondary antibodies (1:2,000, 1 h; Promega), and developed in Western Blue (Promega). For immunohistochemistry, excised eyes were fixed in 4% paraformaldehyde overnight at 4°C. After washing, permeabilization (0.2% Triton X-100), and cryoprotection by sucrose impregnation (10%→20%, 2 h each, then 30% overnight at 4°C), the eyes were embedded in gelatin (7.5% + 15% sucrose). The blocks were frozen at −80°C, equilibrated in the cryostat (−25°C), and sectioned at 7–12 µM. The sections were mounted onto subbed glass slides (Weaver solution). After the gelatin was dissolved in PBS at 36°C, the slides were incubated with primary antibodies (1:500, 2.5 h), followed by Alexa Fluor 546–conjugated secondary goat anti-rabbit antibodies (1 h, 1:200; Molecular Probes) before mounting in 50% glycerol/PBS, covering, and sealing with transparent nail polish. The slides were viewed in a fluorescence microscope (Zeiss Axio Observer). For single-cell immunocytochemistry, isolated photoreceptors plated onto concanavalin A–treated coverslips were dipped in 2% paraformaldehyde for 10 min, permeabilized, and treated as described above.

Generation of the transcriptome of the retina of *Pecten*

The eyes of nine animals were used to microdissect ~300 retinae, and total RNA was extracted (Ambion RN-Aqueous-Micro kit), pooled, and EtHO-precipitated. A library of cDNA was generated and normalized (Bio S&T) and subjected to Roche 454 massively parallel pyrosequencing with GS FLX Titanium-series reagents (Cornell Core Laboratory Center–Genomics, Ithaca, NY); this produced ~7×10^8 primary reads (mean length, 325 bp). The collection was assembled by Roche GS De Novo Assembler at the Bay Paul Center (Marine Biological Laboratory, Woods Hole, MA), resulting in ~44×10^3 isotigs, which, as a preliminary annotation step, were examined by BlastX against the NCBI Reference Sequence nonredundant protein database.

Molecular cloning

For PCR amplifications, *Pecten* retina cDNA was obtained from poly-A mRNA isolated by oligo dT–conjugated magnetic microbeads (Dynal). For reverse transcription, we used the SMART RACE kit (Clontech), which yields 5′ and 3′ cDNAs ready for rapid amplification of cDNA ends (RACE). PCR reactions were performed on an M&J Research DNA Engine cycler; amplicons were purified as needed (Qiagen). For product extension, we used nested RACE reactions. Upon obtaining overlapping sequences that jointly spanned full-length clones (as assembled with the CAP contig assembly routine, BioEdit) a single end-to-end run was conducted to rule out spurious amplification of non-contiguous cDNAs. PCR products were either gel-purified and sequenced directly (Genewiz) or ligated into a sequencing vector (Promega pGEM-T Easy TA); in the latter case, white colonies of chemically transformed *Escherichia coli* (JM-109) grown in ampicillin agar dishes containing isopropyl β-D-1-thiogalactopyranoside and X-Gal were cultured in selective LB medium and checked by colony PCR before extracting and purifying plasmid DNA, which was subjected to restriction analysis before sequencing.

In situ hybridization

Probe generation. Digoxigenin-labeled RNA probes were synthesized by two approaches. (a) A PCR product obtained with Taq polymerase was purified, restricted, and directionally ligated into a dual-promoter expression vector (either pGEM-T Easy [Promega] or pBluescript II SK [Stratagene]), and used to transform *E. coli*. The plasmid was then linearized with either SpeI or SacII. (b) Alternatively, DNA template was directly created by PCR with modified primers in which either a T7 or a Sp6 promoter sequence was added as a 5′ overhang. All the products were verified by sequencing. Labeled sense or antisense riboprobes were synthesized in vitro, by incubating the template in digoxigenin labeling mix (Roche) with T7 or SP6 RNA polymerase (2 h at 42°C). The probe was EtOH-precipitated, dried, and resuspended in diethyl pyrocarbonate H_2O; the concentration was determined spectrophotometrically before dilution in hybridization buffer as a 10× stock, to be stored at −20°C. A dot-blot was performed in a nylon membrane to determine labeling efficiency; to this end, dots of varying dilutions of the probe were incubated with anti-digoxigenin antibodies and developed in Western Blue (Promega).

Probe detection. The procedure for in situ hybridization is based on Shimamura et al. (1994) with few modifications. In brief, samples were sequentially washed in PBS, methanol, and PBS + Tween 20 (PTw), and treated with proteinase K (20 µg/ml). After refixing (0.2% gluteraldehyde + 4% paraformaldehyde) and prehybridization (45 min at 60°C), the probe was added (2 µg/ml), and the slides were coverslipped (hybrislips; Grace Bio Labs) and incubated overnight at 60°C in a hybridization oven (Boekel). Samples were subsequently washed repeatedly and incubated with 100 µg/ml RNase A and 100 U/ml RHase T1 in NTE (0.5 M NaCl, 10 mM Tris, pH 8.0, and 1 mM EDTA). Finally, after additional washes, they were blocked (0.1% Tween, 2 mM levami-

sole, and 2% Boehringer Mannheim Blocking Reagent, 30 min) and incubated overnight with anti-DIG AP antibody (1:2,000, room temperature), before detection with AP substrate solution (Roche).

RNA interference

Double-stranded RNAs were synthesized by Invitrogen; two target sequences were selected for the putative photopigment of ciliary photoreceptors (5′-GAAGAT CCGTCAGACGTCCAATCAA-3′ and 5′-CAACTCGAC ATTTCGTGATTCCTTA-3′), which were used in a 1:1 mix, and one for the α-subunit of the G_o heterotrimeric G-protein (5′-UCCUAUCGUGUAUGCUCUCTT-3′). These were selected on the basis of the complete coding sequence of the two target transcripts, after scrutinizing several dozens of candidates for the presence of suitable motifs (Reynolds et al., 2004; Jagla et al., 2005) and ascertaining their uniqueness by a BLAST search. The probes were fluorescently labeled at the 5′ end with either fluorescein (G_o) or Alexa Fluor 546 (pScop2). To introduce the small interfering RNA (siRNA) into photoreceptor cells, excised retinae were placed in 1-mm-gap electroporation cuvettes in the presence of 0.5–1 µM siRNA (omitted in controls, and replaced with 10 kD dextran-rhodamine; Sigma-Aldrich) and allowed to equilibrate for 5 min. The electroporation solution contained 590 mM sucrose, 72.7 mM NaCl, 14.5 mM KCl, 23.64 mM $MgCl_2$, 3.64 mM Hepes, 118.2 mM Tris, and 9.1 µM $CaCl_2$, pH 7.5. The high concentration of sucrose was empirically determined and served a dual purpose: (a) increasing the density so that the retinae did not sink to the bottom, for better control of exposure to the electric field, and (b) decreasing conductivity to reduce Joule heating. A BTX ECM 830 electroporator delivered either two 30-ms square pulses, 40 V, 5 s apart (for pScop2-siRNA) or three 30-ms pulses, 25 V, 1 Hz (G_o-siRNA). After 5 min, the retinae were transferred to culture medium (DMEM with added salts to mimic the ionic composition of seawater, supplemented with 1 g/liter glucose, 100 U/ml penicillin, and 100 µg/ml streptomycin) and cultured at 15°C. For testing, retinae were enzymatically treated as described in the Cell dissociation and recording section, and dissociated ciliary photoreceptors were screened by fluorescence microscopy for the incorporation of the probe before performing whole-cell recordings.

RESULTS

Cloning of the opsin of distal photoreceptors of *Pecten irradians*

The first goal was to obtain the molecular identity of the photopigment of ciliary photoreceptors of *Pecten*. Exploiting the phylogenetic proximity between *Pecten irradians* and *Mizuhopecten yessoensis*, the predicted protein sequence of Scop2 (Kojima et al., 1997) was used as a query in a tBlastn search of the primary reads of the transcriptome of *Pecten* retina. At this stage, we chose to rely on the collection of primary reads—rather than assembled contigs—in order to identify regions of high representation (six or more overlapping reads) and 100% concordance, thus minimizing uncertainty in primer design. 11 high-scoring initial hits were assembled into a single contig; the end regions were in turn used to search the database again, eventually extending the set to 29 overlapping sequences that apparently represent a single transcript. Suitable stretches were selected and fed to Primer3 for oligonucleotide design, and candidate sequences were further scrutinized for melting point matching, secondary structure, and dimerization (OligoCalculator). Nested PCR reactions yielded the expected products, as confirmed by gel electrophoresis (Fig. 1 A) and subsequent sequencing; these were followed by design of new, outward-facing primers and nested RACE extensions (Fig. 1 B), which resulted in a full-length clone. The nucleotide sequence obtained includes a long open reading frame, translating to a predicted polypeptide of 407 aa (Fig. 1 C). A ClustalW alignment with the sequence of *Mizuhopecten* Scop2 shows a high degree of similarity at both the amino acid level (61% identity) and the nucleotide level (66%). A Blastp search of the NCBI nonredundant protein database yielded, in addition to Scop2 (e-value 2e-171), the other members of the novel opsin group that has been proposed to couple to G_o (namely, those of sea urchin, oyster, and the two isoforms of amphioxus). Hydrophobicity analysis of the amino acid sequence using the Kyte–Doolittle algorithm (13-aa window width) indicated the presence of seven transmembrane domains (Fig. 1 D). As was anticipated, the obtained sequence exhibits a critical residue for the binding of the chromophore: by aligning its sequence with canonical photopigments such as bovine rhodopsin, NinaE (the main rhodopsin of *Drosophila*), and its close relative *Mizuhopecten* Scop2 (UniProt accession nos. P02699, P06002, and O15974, respectively), a lysine was found in a highly conserved stretch of the seventh transmembrane domain (Fig. 1 D). This corresponds to lysine 296 of the bovine form (319 in NinaE, 286 in Scop2 of *M. yessoensis*, and 288 in pScop2 of *P. irradians*), known to establish a Schiff base linkage with 11-cis-retinal. The results therefore indicate the presence of an orthologue of Scop2 in the retina of *Pecten*, henceforth referred to as pScop2 (GenBank accession no. MG674154).

pScop2 localization

Localization of the transcript was assayed by in situ hybridization. Digoxigenin-labeled RNA probes, 1354 bp in length, were generated with primers 169fwd and 1523rev incorporating promoter sites, and directly synthesized from PCR templates. Hybridization assays were conducted on 12-µm-thick formaldehyde-fixed trans-

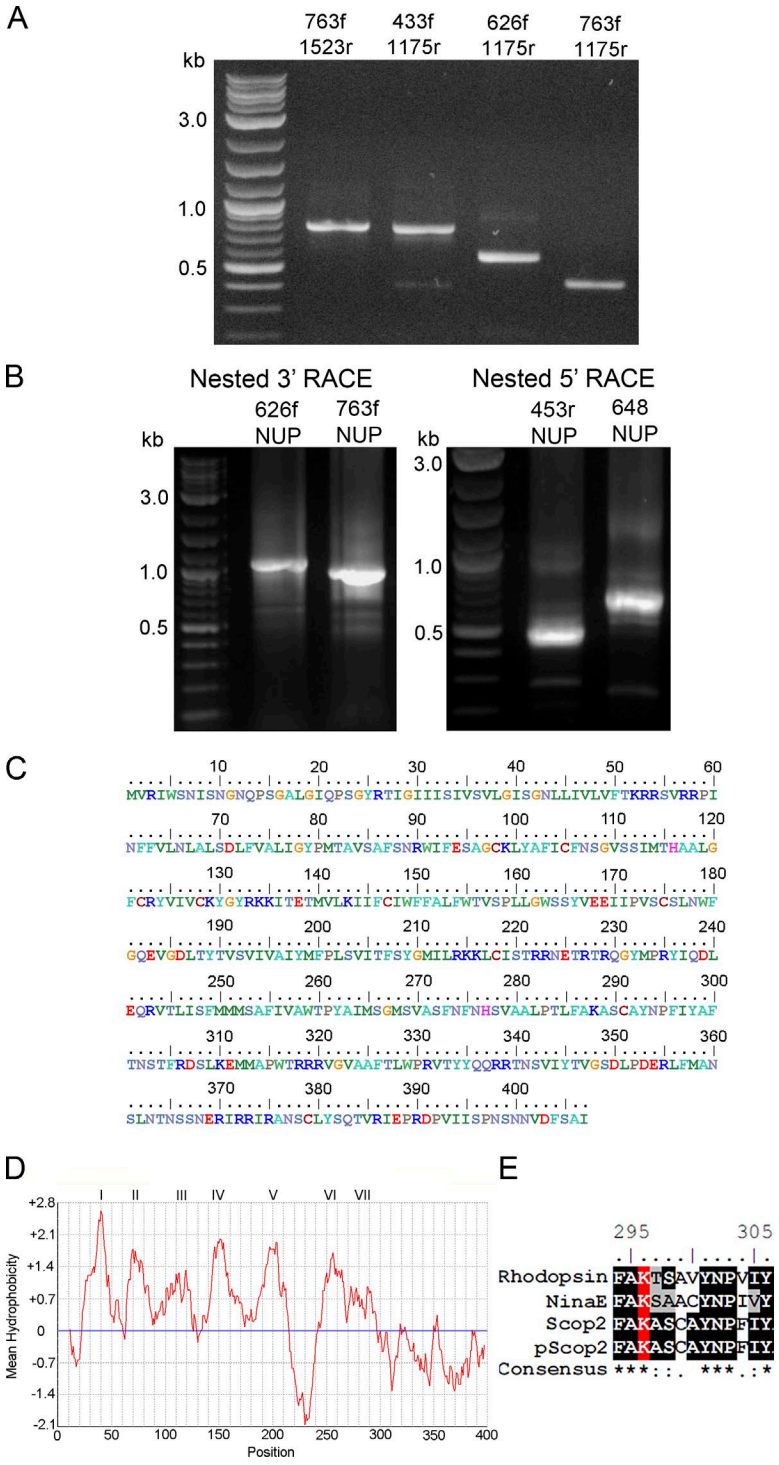

Figure 1. **Cloning the photopigment of the ciliary photoreceptors of the distal retina of *Pecten*.** **(A)** Ethidium bromide–stained agarose gels of the products of PCR reactions with gene-specific primers, which yielded amplicons of the predicted size. **(B)** Nested RACE reactions provided extensions to the 5′ and 3′ ends. **(C)** The full-length transcript obtained has 1647 bp, with a open reading frame that translates to a 407-aa polypeptide. **(D)** Hydrophobicity profile suggests the presence of seven putative membrane-spanning regions. **(E)** Alignment of the chromophore-binding region of bovine rhodopsin and NinaE (*Drosophila* rhodopsin), with *Mizuhopecten* Scop2 and *Pecten* pScop2. The critical lysine in the seventh transmembrane domain, which forms a Schiff-base linkage with retinal, is conserved (highlighted in red).

verse cryosections of isolated retinae. Fig. 2 A shows that a distinct staining pattern was obtained, with the antisense probe targeting selectively the distal retinal layer, which is comprised of the ciliary photoreceptors; labeling was entirely absent when sense riboprobe was used.

Having localized pScop2 mRNA transcripts in the distal retina, the presence of the protein was ascertained by immunodetection. To this end, custom-made, affinity-purified anti-pScop2 antibodies were first assayed in Western blots of *Pecten* retinal lysate. Fig. 2 B shows that a single prominent band was obtained, with an apparent mass of ~50 kD, a figure that compares favorably with the molecular weight calculated from the predicted amino acid sequence (46.2 kD). The slightly larger size and somewhat diffuse appearance of the band may indicate different states of posttranslational modification, such as glycosylations, common among opsins (Murray et al., 2009). This antibody was subsequently used

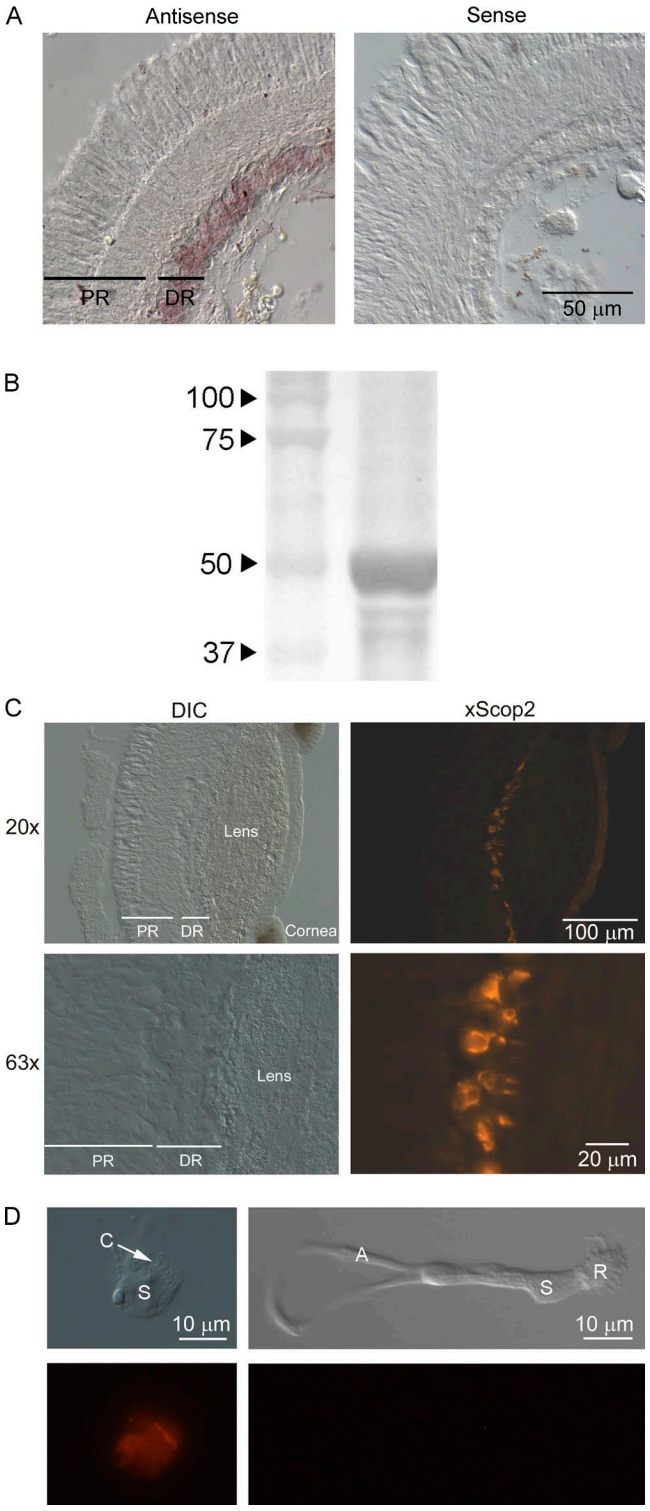

Figure 2. **Localization of pScop2 in the double retina of *Pecten*. (A)** In situ hybridization in cryosections of isolated, fixed retinae incubated with digoxigenin-labeled sense or antisense riboprobes. After hybridization, transcripts were detected using AP-conjugated anti-DIG antibody. Left: The antisense-treated retinae show selective staining in the distal layer (DR), where the ciliary photoreceptors are located, but no labeling in the proximal retina (PR), where microvillar photoreceptors are found. Right: No staining at all appeared in the retinae incubated with the sense probe. **(B)** Western blot of retinal lysate using anti-pScop2 antibody. Proteins separated by SDS-PAGE (8%) before transferring to nitrocellulose membrane. A prominent band is visible near 50 kD, the predicted weight of pScop2. **(C)** Immunohistochemistry to localize pScop2 in eye slices; secondary antibodies were conjugated to Alexa Fluor 546. The lefthand panels show Nomarski images at two magnifications, and the righthand panels show the corresponding fluorescence microscopy images. Immunofluorescence is confined to discrete cells of the distal retina. DIC, differential interference contrast. **(D)** Immunocytochemistry in isolated cells. The retina was enzymatically dissociated, and the cell suspension was plated onto concanavalin A–treated coverslips before incubation with antibodies. The two classes of photoreceptors are recognizable by their distinct morphology; only the ciliary photoreceptors are immunopositive for anti-pScop2 antibody and display an accumulation of the opsin in the region of the ciliary appendages.

to localize the protein in immunohistochemical assays, using secondary antibodies conjugated to Alexa Fluor 546. Fig. 2 C shows both Nomarski and fluorescence micrographs of *Pecten* eye cryosections in which only the cells of the distal retina are distinctly labeled. Control sections, in which the primary antibody was omitted, were completely devoid of labeling (not depicted). To garner further information on the expression pattern, retinae were enzymatically dissociated and processed for immunocytochemistry, allowing unambiguous morphological recognition of the cell types. Fig. 2 D (left) shows an isolated, identified ciliary photoreceptor decorated by anti-pScop2 antibodies, the staining being especially strong in the cilia; in contrast, an isolated microvillar photoreceptor (right) is devoid of label.

Functional demonstration that pScop2 is the ciliary photopigment

The clone that was obtained from *Pecten* ciliary photoreceptors is closely related to the one reported by Kojima et al. (1997) and groups with the other members of this novel opsin subclass that were subsequently uncovered by genome sequence analysis. However, to this date there have been no functional data attesting that such molecules indeed function as photopigments. Exploiting the fact that *Pecten* constitutes a well-developed system for single-cell physiological measurements, we sought such supporting evidence by examining the consequences of interfering with pScop2 in native ciliary photoreceptors.

The initial strategy was to dialyze intracellularly the anti-pScop2 antibodies while monitoring the photocurrent elicited by repetitive flashes. This effort seemed justified because the epitope maps to residues 221–239 in the predicted protein sequence; according to the hydropathicity profile, this stretch is part of the connecting loop between α-helices 5 and 6, a likely site of interaction between opsins and effector G-proteins (reviewed by Shichida and Yamashita, 2003). However, we failed

to observe a consistent depression of the light response amplitude compared with control cells (not depicted). Two factors—not mutually exclusive—could account for the negative results: one is that the antibodies may not be functional; another is that the photocurrent may be a poor criterion to gauge the amount of functional photopigment, because in visual receptors rhodopsin expresses at a vast molar excess with respect to all other signaling elements (e.g., Pugh and Lamb, 1993), and the message from the activated photopigment is subject to great amplification. As a consequence, even substantial interference with the pigment population may not significantly alter the amplitude attained by the photocurrent. We turned therefore to siRNA as a means to reduce pScop2, and to a physiological response that scales linearly with the amount of photopigment present. The maximum charge displacement during photoisomerization fills the requirement (see Discussion). To quantify this parameter, one must measure the early receptor current (ERC). Fig. 3 A illustrates the membrane current elicited by an intense broadband light stimulus in an isolated ciliary photoreceptor of *Pecten* voltage-clamped to −40 mV. The large outward photocurrent (I_L) is mediated by the opening of K-selective ion channels (Gomez and Nasi, 1994a) and is preceded by a small, rapid hump (rectangle, shown at an enlarged scale in the inset). Identification of such early transient as a photopigment displacement current is supported by the fact that (a) it is very rapid: latency 0.3 ± 0.08 ms SEM, time to peak 3.1 ± 0.92 ms, $n = 6$ (after correcting for actual shutter opening time and photocurrent time shift caused by the analogue filter; see Materials and methods); (ii) it appears only at light intensities that are saturating for the late photocurrent, i.e., a regimen that causes massive, synchronous stimulation of rhodopsin; (iii) it survived application of the K-channel blocker 4-aminopyridine (20 μM; Fig. 3, B and C), which is an effective antagonist of the light-activated conductance of these cells (Gomez and Nasi, 1994b); and (iv) it is largely unaffected by changes in ionic driving forces, whereas, as V_m is hyperpolarized, the late photocurrent is gradually reduced until vanishing at −80 mV, close to E_K (Fig. 3 D). In addition, because of the large spectral shift between rhodopsin (R, $\lambda_{max} \approx 500$ nm; McReynolds and Gorman, 1970b; Cornwall and Gorman, 1983) and metarhodopsin (M, $\lambda_{max} \approx 576$ nm), photopigment state distribution can be manipulated by chromatic adaptation before the test flash, and this is reflected in the size and polarity of the early component (Fig. 3 E). This feature was also exploited to reset photopigment state with a red light ($\lambda > 630$ nm, 3 s) applied 1 min before each ERC recording, to ensure reproducibility of the ERC over repeated trials.

To assess the effects of pScop2 RNA interference (RNAi), ERCs were elicited by brief test flashes (6 ms) of 470-nm peak wavelength (near the optimum value in the photo-equilibrium spectrum to yield the largest net R→M transition; Cornwall and Gorman, 1983). The total amount displaceable charge can be gauged from the maximum value of the integral of the ERC. Fig. 4 A illustrates a family of ERC traces elicited by flashes of increasing intensity in a control cell. Each current record was integrated, and the resulting values are plotted in Fig. 4 B; the ensemble clearly shows a saturating behavior. Data points were least-squares fitted by an exponential function, the asymptote of which yields the desired estimate for the maximal photoisomerization charge, which reflects the total amount of photopigment. After siRNA introduction, a suitable temporal window must be interposed, before a phenotype becomes manifest. To preserve cell viability during that time period, organotypic culture proved far more robust than culturing dissociated cells: an excised retina can be maintained for 2–3 d with few special precautions, and upon enzymatic dispersion the photoreceptors look indistinguishable from freshly obtained cells and retain their normal light responsiveness. In contrast, cultured dissociated photoreceptors begin to de-differentiate within 1 d, and many of them subsequently die (unpublished data). Therefore, we opted for electroporating the intact retinae and dissociating them only before the electrophysiological test (see also Matsuda and Cepko, 2004). Before evaluating pScop2-RNAi, pilot experiments were conducted to optimize electroporation parameters, using 10 kD dextran-conjugated rhodamine (Molecular Probes) to mimic siRNA (~13 kD); 24–48 h later, photocurrents were examined by whole-cell patch recording. We found conditions that met two indispensable criteria: (1) a fraction of the cells showed incorporation of the fluorescent probe, attesting the efficacy of the electroporation, and (2) labeled photoreceptors remained light-sensitive (amplitude and the light intensities producing half-maximal responses were not altered, compared with control cells), indicating that the treatment is not unduly harsh. We then examined the effects of pScop2-siRNA on the ERC, compared with control retinae electroporated in the presence of dextran-rhodamine; we also exploited the unique dual nature of *Pecten* retina, which presents a second, proximal layer of conventional microvillar photoreceptors (Barber et al., 1967; Gorman and McReynolds, 1969), and assessed the impact of the pScop2 siRNA on the ERC of these cells, which express an entirely different rhodopsin (Kojima et al., 1997) and thus serve as ideal negative controls. Post-electroporation culturing periods, before enzymatic dispersion, were typically 24–48 h; longer incubation times up to 72 h were tested, but did not yield any additional benefit. Target cells were selected by fluorescence before conducting the electrophysiological tests. Fig. 4 C shows traces of the ERC recorded in a control photoreceptor and in one treated with pScop2 siRNA; in the latter, the de-

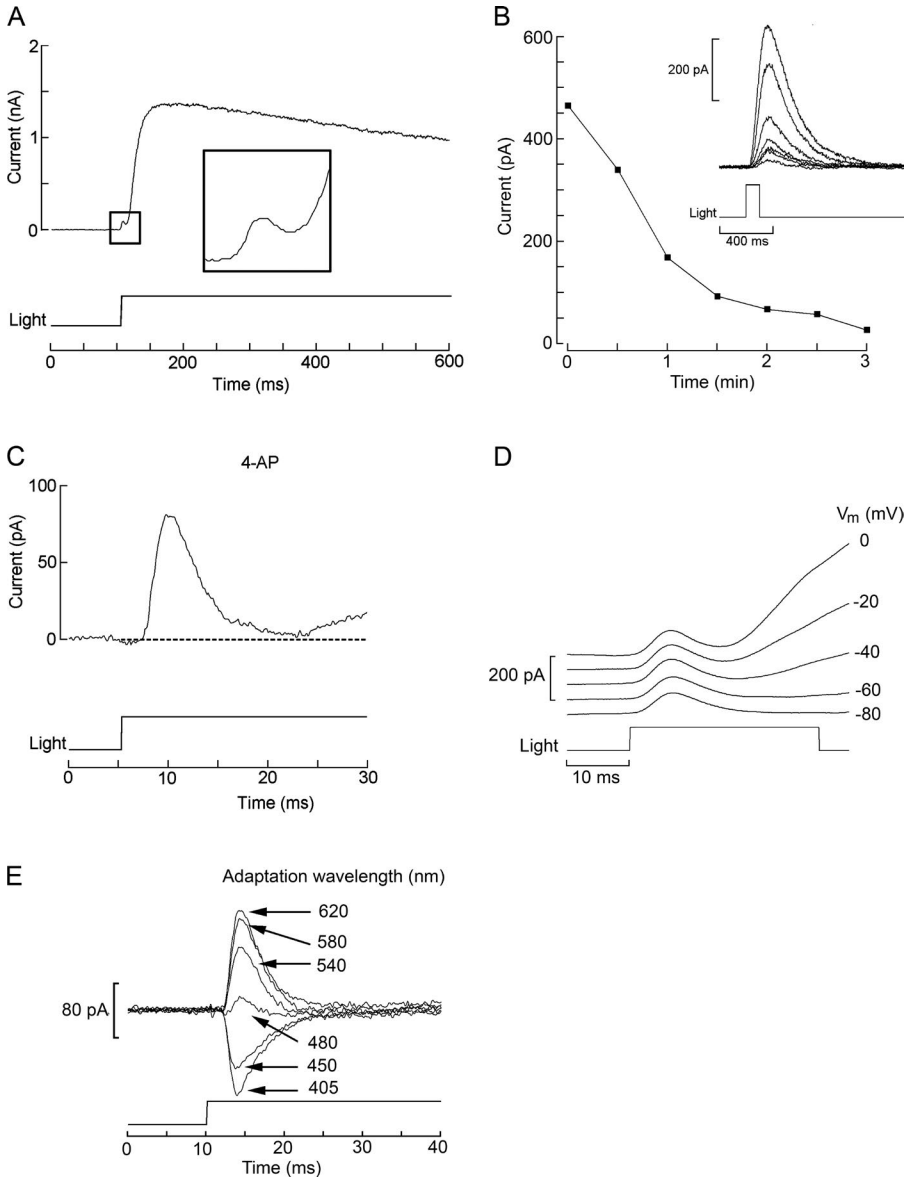

Figure 3. **Identification of the ERC arising from photopigment isomerization in ciliary photoreceptors. (A)** Whole-cell recording of membrane current in an isolated cell voltage-clamped at −40 mV and stimulated with an intense light step (4.1×10^{17} photons $\cdot$ s^{-1} $\cdot$ cm^{-2}). Illumination evoked the characteristic outward current mediated by K-channels, but its activation was preceded by a brief, much smaller transient (rectangle and inset) that partially overlaps with the photocurrent rising phase. **(B)** Progressive reduction of the photocurrent evoked by moderate flashes (7.3×10^{15} photons $\cdot$ s^{-1} $\cdot$ cm^{-2}, 100 ms), during superfusion with the K-channel blocker 4-aminopyridine (20 µM). **(C)** The early component can be isolated in the presence of 4-aminopyridine (4-AP). Under these conditions, its falling phase is fully resolved, with little contamination by the late photocurrent. **(D)** Manipulations of membrane voltage greatly impact the late light–evoked current but leave the early component largely unaffected. The membrane potential was set at the specified value a few seconds before delivering the light stimulus. At −80 mV, near the calculated equilibrium potential for K ions, the late photocurrent virtually disappears. Duration of light flashes, 30 ms. **(E)** The size and polarity of the early component is determined by prior chromatic adaptation. The cell was illuminated with monochromatic light (three-cavity filters, intensities 10^{14} to 2.5×10^{15} photons $\cdot$ s^{-1} $\cdot$ cm^{-2}) for several seconds to reach photoequilibrium of the pigment state, before being stimulated with a fixed high-intensity test stimulus of white light. When the adapting light was of long wavelength, the early component had an outward direction, but became inward with chromatic adaptation to progressively shorter wavelengths. The holding potential was kept at −40 mV throughout. Light intensity for test flashes in C–E, 5.8×10^{17} photons $\cdot$ s^{-1} $\cdot$ cm^{-2}.

pression of the photoisomerization current is dramatic. The bar graph in Fig. 4 D summarizes the data, pooling the results for several experimental versus control ciliary and rhabdomeric cells. pScop2-siRNA treatment significantly decreased the photodisplaceable charge in ciliary photoreceptors ($P < 0.0029$, *t* test, $n = 8–11$ per group), whereas it produced no discernible effect on the ERC of microvillar photoreceptors. This indicates that pScop2 is isomerized by light.

We next sought evidence that pScop2 engages the light-signaling cascade (as there are groups of opsins that photoisomerize but are not involved in signaling; Terakita, 2005). The main hurdle was that the downstream physiological process to be measured must also be strongly sensitive to absolute amounts of photopigment, and this rules out the regular light response. In contrast, the prolonged aftercurrent (PA) that occurs in photoreceptors endowed with a bistable photopigment serves the purpose. This phenomenon has been documented in various species (reviewed by Hillman et al., 1983; see Discussion), in which intense chromatic illumination causes a sustained light response, thought to arise from the net accumulation of metarhodopsin, causing photo-excitation shutoff mechanisms to satu-

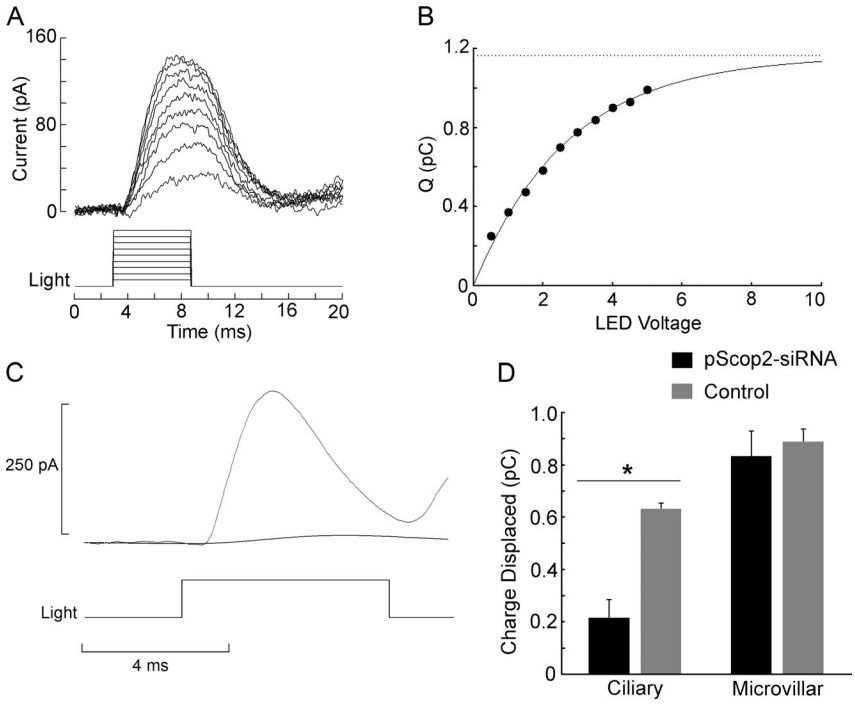

Figure 4. **pScop2 is photoisomerized by light and underlies the ERC. (A)** ERCs evoked by flashes of increasing intensity (470 nm, 6 ms in duration, 1.3×10^{17} to 9.1×10^{17} photons $\cdot$ $s^{-1} \cdot \cdot cm^{-2}$) in a ciliary photoreceptor voltage-clamped at −40 mV. Between trials, a 5-s period of red illumination (620 nm) was interposed 1 min before the subsequent test flash, to reset the photopigment to the R state. **(B)** Saturation of the charge displaced by illumination. The amount of charge displaced at each stimulus intensity was obtained by integrating the corresponding current traces of A. An exponential function was least-squares fitted to the data points to extract the estimated asymptote; this represents the maximum photoisomerization charge, which in turn reflects the total amount of photopigment in the cell ($r^2 = 0.992$). **(C)** Comparison of the ERC obtained in a control ciliary photoreceptor and one previously treated with pScop2-siRNA; the treatment greatly attenuated the ERC. Test flash, 7.9×10^{17} photons $\cdot$ $s^{-1} \cdot cm^{-2}$, 6-ms duration. **(D)** Mean total photoisomerization charge under control and RNAi conditions, for the two photoreceptor types in the double-retina of *Pecten*. Before dissociation and electrophysiological testing, the retinae were subjected to electroporation in the presence of either pScop2-siRNA or fluorescent dextran as a control and cultured for 24–48 h. Only in ciliary photoreceptors did the RNAi treatment depress the amount of photoisomerization charge (*, $P < 0.01$, *t* test). Error bars indicate SEM.

rate. In the case of *Pecten* ciliary photoreceptors, such prolonged aftereffects can be elicited by short-wavelength illumination (Cornwall and Gorman, 1983; Gomez and Nasi, 1994b; Gomez et al., 2011). Fig. 5 A illustrates the time course of the light response evoked by a blue light (bandpass interference filter 400–500 nm); although with moderate light intensities, the photocurrent decays shortly after the termination of the stimulus, as intensity is raised a progressively more sustained tail appears. To corroborate that the phenomenon is a consequence of accumulation of activated photopigment, Fig. 5 (B and C) show repetitively evoked PAs that are terminated in an intensity-dependent fashion by the application of a long-wavelength light, which induced the reverse M→R transition. We reasoned that if pScop2 stimulates the light-transduction cascade, its knockdown must be reflected in a reduced likelihood of evoking PAs because shutoff mechanisms ought to be able to cope with the decreased amount of photopigment activated by a saturating light. Fig. 5 D shows the effect of a supersaturating flash of blue light (470 nm) in a control electroporated cell, causing the expected sustained activation of an outward photocurrent that persisted with only a modest decay for the 10-s duration of the recording. In contrast, similar chromatic stimulation applied to a photoreceptor electroporated with pScop2-siRNA evoked a photocurrent that rapidly declined toward baseline. To provide a quantitative index of the effect, we calculated the ratio between the amplitude of the photocurrent at 10 s versus at the peak, for a group of experimental and control photoreceptors; the obtained averages (0.11 ± 0.03 SEM, $n = 12$, and 0.36 ± 0.05, $n = 9$, respectively) differed in a statistically significant way ($P = 0.012$, *t* test). These observations attest the competence of pScop2 to activate the light-signaling pathway. Collectively, the observations that pScop2 knockdown depresses both ERCs (the earliest manifestation of photoexcitation) and PAs (which engage light-dependent ion channels) strongly support the notion that this molecule forms the functional visual pigment of *Pecten* ciliary photoreceptors.

pScop2 operates via G_o

Having garnered evidence for the molecular identity of the bistable photopigment of ciliary photoreceptors of *Pecten*, we sought to strengthen the notion that this novel class of light-sensing molecules indeed signals through G_o. This proposition was previously based

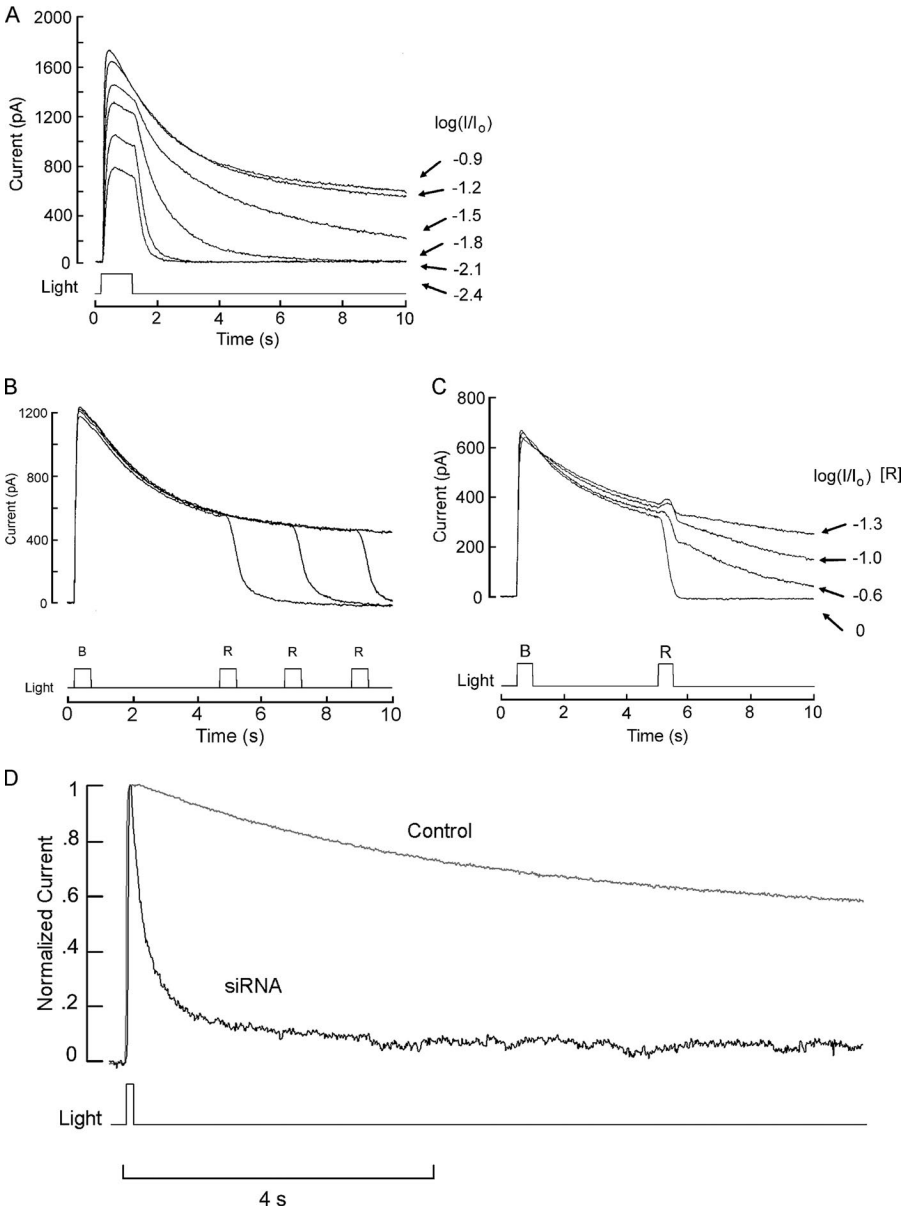

Figure 5. **PAs reveal that pScop2 couples to the light-signaling cascade. (A)** Progressive development of prolonged outward aftercurrents as the intensity of stimulating blue light (delivered every 2 min) is increased. Unattenuated light intensity, 5.3×10^{17} photons $\cdot s^{-1} \cdot cm^{-2}$; attenuation factor, achieved by neutral-density filters, indicated at the right. The cell was voltage-clamped at −30 mV. After each trial, a 3-s period of red adaptation was applied to ensure constancy of initial distribution of photopigment state. **(B)** Termination of the PA by photoconversion of activated rhodopsin to the quiescent state. A bright blue flash ($\lambda < 500$ nm, 500 ms) of constant intensity (5.3×10^{17} effective photons $\cdot s^{-1} \cdot cm^{-2}$) was presented every 3 min, evoking a PA with nearly identical time course. In each case, a second flash of red light ($\lambda > 630$ nm; 2.9×10^{16} photons $\cdot s^{-1} \cdot cm^{-2}$) was presented after a variable delay, causing a rapid reset of the sustained photocurrent back to the baseline level. **(C)** Intensity dependence of the PA shutoff. A 500-ms blue light (5.3×10^{17} photons $\cdot s^{-1} \cdot cm^{-2}$) was applied every 2 min, followed 4.5 s later by a 500-ms red light, the intensity of which was progressively increased, as indicated (unattenuated intensity, 2.9×10^{16} photons $\cdot s^{-1} \cdot cm^{-2}$). The degree of suppression of the sustained photocurrent was monotonically related to the amount of red stimulation, as expected from the extent of the concomitant M→R conversion. **(D)** Treatment with pScop2 siRNA depresses the PA. A chromatic stimulus that in a control photoreceptor produces a sustained activation of the photocurrent (100 ms, 3.1×10^{17} photons $\cdot s^{-1} \cdot cm^{-2}$), evokes only a transient response in a cell electroporated with siRNA (100 ms, 6×10^{17} photons $\cdot s^{-1} \cdot cm^{-2}$).

only on colocalization within the retina (Kojima et al., 1997) and pharmacology (Gomez and Nasi, 2000). A more direct confirmation would entail identifying such G_o and assessing the effects of selectively manipulating it. To this end, primers were initially designed on the basis of the G_o of several invertebrates (*M. yessoensis*, BAA22220; *Octopus vulgaris* AB025781; *Limnaea stagnalis* Z15094.1; *Helisoma trivolvis* L18921). A first PCR amplification yielded a stretch of 114 nucleotides which served to generate additional primers for nested RACE reactions, which eventually yielded a full-length clone (GenBank accession no. MG674155). The predicted protein is comprised of 357 aa and is 99% identical to that of *Mizuhopecten* (Kojima et al., 1997), with only three discrepancies. Fig. 6 A illustrates a ClustalW alignment against the top-ranking $G_o\alpha$ protein sequences. A cysteine in the fourth position from the carboxy terminus is the hallmark of susceptibility to ADP ribosylation, which dovetails with prior observations that the light response of *Pecten* ciliary photoreceptors is susceptible to inhibition by pertussis toxin (Gomez and Nasi, 2000). Analysis of the transcriptome indicated that the obtained clone is the sole isoform of G_o expressed in the retina.

In situ hybridization was subsequently used to localize G_o. We tested a whole-mount approach using entire eyecups (cornea and lens removed) in which the retina remains attached by the optic nerve. This was designed to reduce losses resulting from the detachment of sections from the glass slides during the hybridization procedure; only after development with the chromogenic substrate were the eyecups embedded, sectioned, and

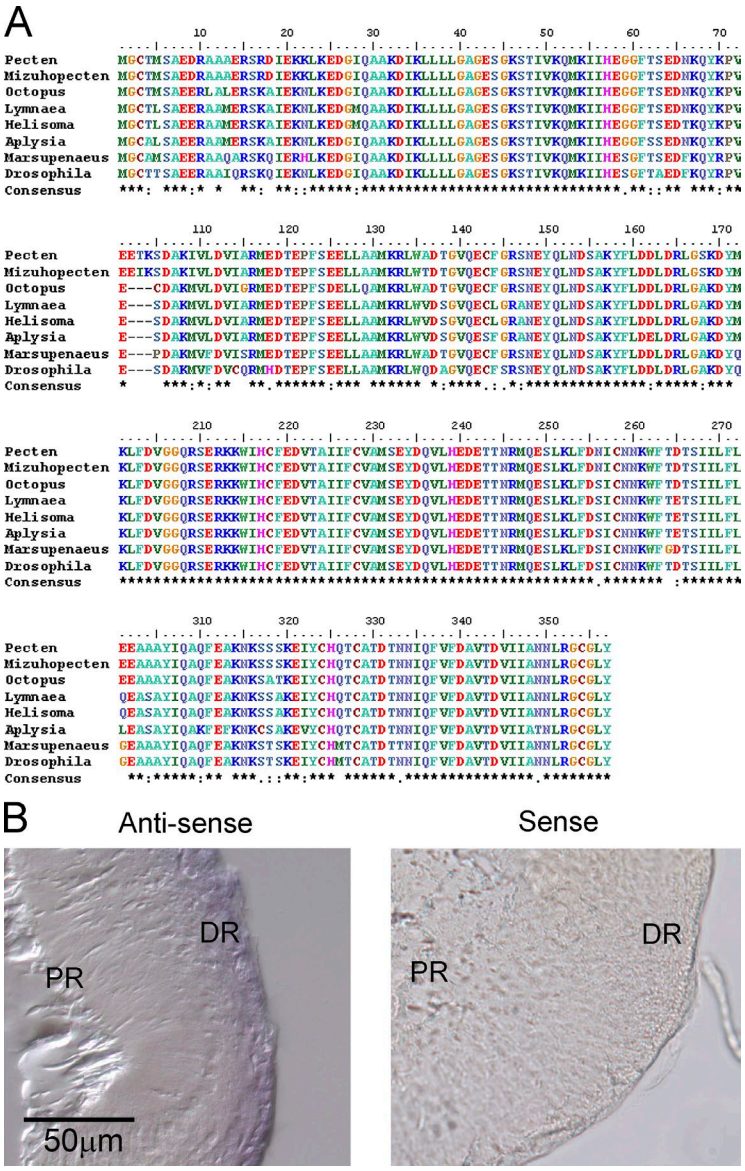

Figure 6. **$G_{o\alpha}$ cloned a from *Pecten* retina cDNA.** **(A)** ClustalW alignment of the predicted amino acid sequence of the full-length clone obtained by PCR, against other known $G_o\alpha$ of mollusks. **(B)** In situ hybridization with digoxigenin-labeled riboprobes targeting $G_o\alpha$. The figure shows a cryosection of an isolated retina. The antisense probe distinctly labeled the distal retinal layer. No discernible staining was obtained with the control sense probe. PR, proximal retina; DR, distal retina.

mounted on microscope slides. Probes were synthesized from linearized plasmids; because the sequence contained no suitable restriction sites for directional ligation into the vector, a 320-bp PCR fragment was generated with EcoRI and HindIII sites introduced at the 5′ ends of the modified primers. Fig. 6 B shows that a distinct staining pattern was observed with the antisense probe, with the distal layer being selectively decorated, whereas there was no discernible staining by the sense probe.

Functional evidence for the specific involvement of G_o in light transduction was sought by an RNAi approach, similarly to the experiments performed with pScop2, described in the previous section. Fig. 7 A shows bright-field and fluorescence micrographs of an isolated ciliary photoreceptor 24 h after electroporation with fluorescein-labeled G_o-siRNA. In Fig. 7 B, superimposed traces of photocurrents evoked by flashes of increasing intensity are compared for a control cell electroporated with dextran-rhodamine and an experimental photoreceptor treated with G_o siRNA; the photocurrent was substantially attenuated. In Fig. 7 C, the bar graph summarizes the results; siRNA treatment (n = 23) significantly depressed the maximum amplitude of the light-evoked current with respect to both untreated, cultured controls (by 74%; n = 7) and dextran-electroporated controls (by 68%; n = 8). The effect was statistically highly significant ($P < 0.01$ in both cases; t test); although in the latter group the mean light response amplitude was somewhat smaller than in cells not subjected to electroporation, the difference turned out not to be statistically significant ($P = 0.18$).

DISCUSSION

A novel class of putative visual opsins that diverge from the canonical forms of both vertebrates and inverte-

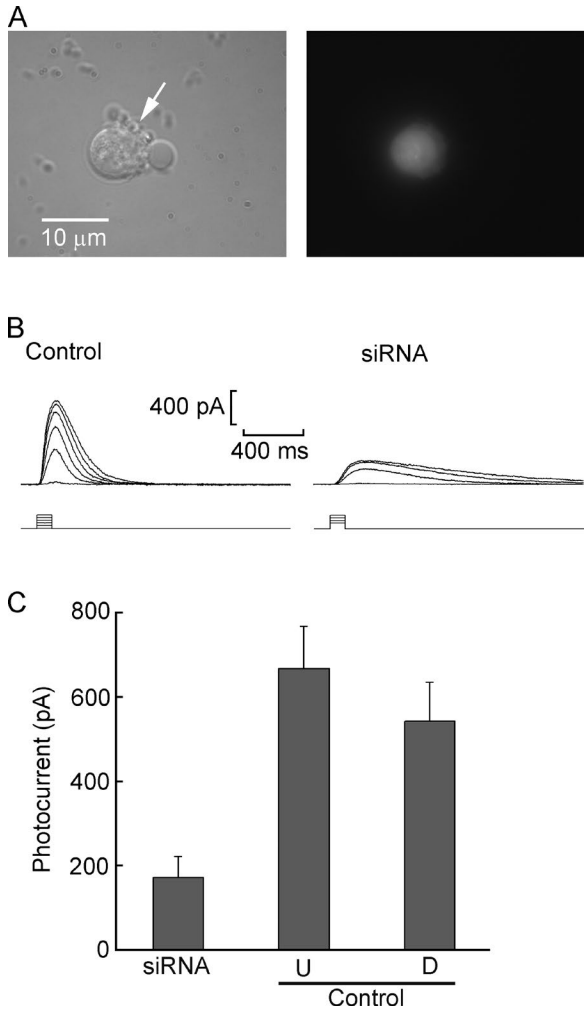

Figure 7. **siRNA against G_o reduces light responsiveness. (A)** Transmitted-light micrograph (left) and fluorescence image (right) of a dissociated ciliary photoreceptor that was electroporated with fluorescein-labeled siRNA. The small spherical protuberances (arrow) are the light-sensitive ciliary appendages. **(B)** Comparison of the photocurrent evoked by progressively brighter flashes (100 ms) in a control cell electroporated with rhodamine-conjugated 10-kD dextran (left) and a photoreceptor electroporated with siRNA targeting G_o (right). Light intensity linearly increased from 1.4×10^{14} to 3.8×10^{15} photons $\cdot s^{-1} \cdot cm^{-2}$; the two dimmest flashes were skipped in the siRNA-treated cell. **(C)** Mean maximal light response amplitude in pooled cells dissociated from retinae treated with siRNA (n = 23), cultured untreated retinae (n = 7), or retinae electroporated with rhodamine-dextran (n = 8). The first group differed significantly from the other two ($P < 0.001$, t test), whereas the differences between the two control groups did not attain statistical significance. U, untreated; D, dextran electroporated.

brates has recently been established by cloning and genome analysis and shown to have a wide phylogenetic distribution. However, the identity of the cells that express these opsins remained uncertain (or, for some species, completely unknown), and no direct evidence had been garnered that such molecules actually form functional photopigments, in either native light-sensitive cells or heterologous expression systems. In the present work, a new member of this group was molecularly identified in the eye of the bay scallop, *Pecten irradians*, and positively localized to the distal retinal layer, which is comprised of ciliary, hyperpolarizing photoreceptors. This model system is unique in that it has been the object of a substantial number of functional studies, which have led to a detailed physiological characterization of its light response (e.g., Gorman and McReynolds, 1969, 1978; Gomez and Nasi, 1994b,a, 2000; del Pilar Gomez and Nasi, 1995). Our results provide strong evidence that the molecule in question, pScop2, indeed constitutes the photopigment that underlies the receptor potential of *Pecten* hyperpolarizing visual cells, linking together for the first time molecular and physiological observations on these uncommon photoreceptors and novel opsins.

To provide the necessary functional support, a criterion sensitive to even moderate variations in the amount of photopigment was needed. Because of the presence of an amplification cascade and the large excess of rhodopsin over other light-signaling molecules, the photocurrent is not ideal: its peak amplitude can remain largely unaffected by a reduction of the level of rhodopsin—unless this is extreme—whereas shifts in sensitivity are subject to variability. We focused first on the charge movement that accompanies photoisomerization, which is linearly related to the photopigment content of the cell. This phenomenon underlies the early receptor potential (ERP), and its counterpart, the ERC, that was first described in mammals (Brown and Murakami, 1964; Cone, 1967) and subsequently reported in amphibians (Hodgkin and Obryan, 1977; Hestrin and Korenbrot, 1990; Makino et al., 1991) and G_q-coupled rhodopsins of arthropods (Lisman and Sheline, 1976) and of prechordates (Ferrer et al., 2012). A robust ERP had also been demonstrated in *Pecten* ciliary photoreceptors by Cornwall and Gorman (1983), who used it to characterize in detail the reversible transitions of the bistable photopigment. Because the ERP reports only rhodopsin conformational changes, it is impervious to the state of all downstream links of the light transduction cascade and of the cell in general; in fact, it survives anoxia (Brown and Murakami, 1964) and formaldehyde fixation (Brindley and Gardner-Medwin, 1966) and can even be measured in artificial bilayers incorporating rhodopsin (Trissl et al., 1977). Our results showed that siRNA targeting pScop2 caused a significant reduction in the total amount of charge that can be displaced by light, the effect being circumscribed specifically to ciliary photoreceptors. Although this outcome indicates that pScop2 undergoes photoisomerization, it does not demonstrate that it is capable of triggering the light-signaling cascade. For example, certain opsin subgroups are found in nonphotosensitive tissues and/or perform nonsensory functions (e.g., photoisomerase), rather

than light transduction (Terakita, 2005). To clarify this point, we exploited another useful property of the model system, its ability to produce PAs in response to chromatic light stimulation. This phenomenon is a consequence of both the thermal stability of the rhodopsin (common to all invertebrates) and the condition that the inactive and active states differ in peak absorption wavelength (which occurs in several, but not all, species; Hillman et al., 1983). Narrow-band illumination can change the pigment distribution, which will asymptotically tend to

$$F_M(\lambda, \infty) = P_R(\lambda) / [P_R + (\lambda) + P_M(\lambda)],$$

where F is the limiting fractional distribution, λ is the wavelength, P is the photosensitivity (i.e., extinction coefficient × quantum efficiency), and the subscripts M and R denote metarhodopsin and rhodopsin, respectively (Hillman et al., 1983). In *Pecten*, short-wavelength illumination can cause a large accumulation of metarhodopsin, resulting in a sustained photocurrent that can last for tens of seconds. Evidence has been provided that saturation of arrestin—which is molarly underrepresented with respect to the photopigment—is the main culprit of the occurrence of the aftercurrent (Gomez et al., 2011). For the present purposes, the important consideration is that PAs (a) are necessarily sensitive to the total amount of photopigment, (b) provide a readout that is distinct from the amplitude of the light response, and (c) implicate the activation of the phototransduction pathway. The reduction of PA after RNAi treatment supports the conclusion that pScop2 is responsible for initiating the signaling activity that leads to the opening of light-dependent ionic channels. In both sets of experiments using siRNA, we did not attempt to estimate protein knockdown (e.g., using the anti-pScop2 antibodies), for the following reasons: (a) the efficiency of transfection, as gauged by fluorescence microscopy, varied across preparations but did not exceed 20%; stronger electroporation pulses intended to increase the yield proved detrimental, significantly compromising cell viability; and (b) within the transfected cells, the mean decrease in photo-isomerization charge was ~60–70% (Fig. 3 E). Under such circumstances, a macroscopic comparison of protein levels between experimental and control preparations would likely fall below the resolution of a Western blot, as the total decrease of pScop2 (i.e., the product of transfection efficiency and the decrease of photoisomerization charge in transfected cells) would be only on the order of 12–14%.

The establishment of pScop2 as a functional photopigment strongly implies that the founding member of this class, which Kojima et al. (1997) identified in the eye of another bivalve mollusk, is a bona fide visual pigment, and lends credence to the notion that more distantly related molecules in echinoderms and prechordates likely perform photoreceptive functions too. However, those animals are devoid of differentiated eyes, and information on the cells that express these opsins is completely lacking, so the particular role of such photopigments in other organisms remains to be investigated.

We also obtained the molecular identity of a G_o of *Pecten* retina, localized it to the ciliary photoreceptor layer, and demonstrated the specific depression of the light response after administration of siRNA. These observations provide strong evidence that, as originally proposed by Kojima et al. (1997), such novel opsins signal through a different subtype of heterotrimeric G-proteins than those that convey the rhodopsin signal in canonical photoreceptors. The results dovetail with previous clues garnered from pharmacological studies (Gomez and Nasi, 2000). A role of G_o has also been proposed in the photoresponse of lizard parietal eye photoreceptors (Su et al., 2006) and extra-ocular receptors of the mollusk *Onchidium verrunculatum* (Gotow and Nishi, 2007), pointing to a relatively widespread representation across taxa. Little is known about the downstream effectors, which may turn out to be assorted: the mobilization of cGMP that underlies photoexcitation in *Pecten* (del Pilar Gomez and Nasi, 1995; Gomez and Nasi, 1997b, 2005) and *Onchidium* (Nishi and Gotow, 1998; Gotow and Nishi, 2002) seemingly reflects light-dependent regulation of its synthesis, suggesting a G_o-regulated guanylate cyclase (Gomez and Nasi, 2000; Gotow and Nishi, 2007), which remains to be identified. In contrast, in the lizard a phosphodiesterase has been implicated (Su et al., 2006). Note that, unlike the well-delimited targets of G_s, G_q, or G_t, the effectors of G_o can be quite diverse (Jiang and Bajpayee, 2009). Because nothing is known about the cells that express this type of opsin in amphioxi and sea urchins, it is unclear whether this divergence of effectors is representative of the split between protostomia and deuterostomia.

In the case of both pScop2 and G_o, the functional consequences of siRNA were evident at 24 h of incubation and failed to increase further at 48 h. This is consistent with observations in other photoreceptors, demonstrating that the cycling of light transduction proteins can be rapid: in fact, in invertebrate photoreceptors a massive turnover of the photosensitive membrane (up to 70%) is paced by the circadian cycle (Chamberlain and Barlow, 1979, 1984).

Our findings, obtained in a system that proved amenable to both molecular and physiological analysis, provide definitive functional support for a third lineage of animal visual pigments with their distinct cognate effectors, after the well-characterized C-opsins and R-opsins. According to sequence analysis, this ancient subgroup diverged very early from other opsins (Terakita, 2005) and can help better understand the evolutionary his-

tory of light-sensing molecules in animals. The experimental confirmation that such photopigments couple to a G_o could also result in a useful new tool for functionally investigating signaling mediated by this heterotrimeric G-protein, which is the most abundant in the nervous system (Jiang and Bajpayee, 2009), but also the least understood in terms of targets, mechanisms, and regulation.

ACKNOWLEDGMENTS

We wish to express our gratitude to Dr. David Mark Welch, Bay Paul Center, Marine Biological Laboratory, for newbler assembly of the transcriptome, to Fabio Echeverry for the massive RNA extraction, and to Juan Manuel Angueyra and Francisca Silva for pilot work to develop the electroporation and the in situ hybridization assays.

Supported by Departamento Administrativo de Ciencia, Tecnología e Innovación (Colcencias; grant FP44842-010-2015) and by Fund for Science.

The authors declare no competing financial interests.

Author contributions: O. Arenas, T. Osorno, G. Malagón, and C. Pulido helped plan the experiments, performed experiments, and contributed to data analysis. MdelP Gomez and E. Nasi were responsible for overseeing the project, planned and performed experiments, contributed to data analysis, and wrote the manuscript.

Anna Menini served as guest editor.

Submitted: 30 October 2017
Accepted: 20 December 2017

REFERENCES

Arendt, D., K. Tessmar-Raible, H. Snyman, A.W. Dorresteijn, and J. Wittbrodt. 2004. Ciliary photoreceptors with a vertebrate-type opsin in an invertebrate brain. *Science.* 306:869–871. https://doi.org/10.1126/science.1099955

Arikawa, K., J.L. Hicks, and D.S. Williams. 1990. Identification of actin filaments in the rhabdomeral microvilli of *Drosophila* photoreceptors. *J. Cell Biol.* 110:1993–1998. https://doi.org/10.1083/jcb.110.6.1993

Barber, V.C., E.M. Evans, and M.F. Land. 1967. The fine structure of the eye of the mollusc Pecten maximus. *Z. Zellforsch. Mikrosk. Anat.* 76:25–312. https://doi.org/10.1007/BF00339290

Brindley, G.S., and A.R. Gardner-Medwin. 1966. The origin of the early receptor potential of the retina. *J. Physiol.* 182:185–194. https://doi.org/10.1113/jphysiol.1966.sp007817

Brown, K.T., and M. Murakami. 1964. A new receptor potential of the monkey retina with no detectable latency. *Nature.* 201:626–628. https://doi.org/10.1038/201626a0

Chamberlain, S.C., and R.B. Barlow Jr. 1979. Light and efferent activity control rhabdom turnover in *Limulus* photoreceptors. *Science.* 206:361–363. https://doi.org/10.1126/science.482946

Chamberlain, S.C., and R.B. Barlow Jr. 1984. Transient membrane shedding in *Limulus* photoreceptors: Control mechanisms under natural lighting. *J. Neurosci.* 4:2792–2810.

Cone, R.A. 1967. Early receptor potential: Photoreversible charge displacement in rhodopsin. *Science.* 155:1128–1131. https://doi.org/10.1126/science.155.3766.1128

Cornwall, M.C., and A.L.F. Gorman. 1983. Colour dependence of the early receptor potential and late receptor potential in scallop distal photoreceptor. *J. Physiol.* 340:307–334. https://doi.org/10.1113/jphysiol.1983.sp014764

de Couet, H.G., S. Stowe, and A.D. Blest. 1984. Membrane-associated actin in the rhabdomeral microvilli of crayfish photoreceptors. *J. Cell Biol.* 98:834–846. https://doi.org/10.1083/jcb.98.3.834

del Pilar Gomez, M., and E. Nasi. 1995. Activation of light-dependent K+ channels in ciliary invertebrate photoreceptors involves cGMP but not the IP3/Ca2+ cascade. *Neuron.* 15:607–618. https://doi.org/10.1016/0896-6273(95)90149-3

del Pilar Gomez, M., and E. Nasi. 2005. Calcium-independent, cGMP-mediated light adaptation in invertebrate ciliary photoreceptors. *J. Neurosci.* 25:2042–2049. https://doi.org/10.1523/JNEUROSCI.5129-04.2005

Ferrer, C., G. Malagón, M.P. Gomez, and E. Nasi. 2012. Dissecting the determinants of light sensitivity in amphioxus microvillar photoreceptors: Possible evolutionary implications for melanopsin signaling. *J. Neurosci.* 32:17977–17987. https://doi.org/10.1523/JNEUROSCI.3069-12.2012

Gomez, M.P., and E. Nasi. 1994a. The light-sensitive conductance of hyperpolarizing invertebrate photoreceptors: A patch-clamp study. *J. Gen. Physiol.* 103:939–956. https://doi.org/10.1085/jgp.103.6.939

Gomez, M.D., and E. Nasi. 1994b. Blockage of the light-sensitive conductance in hyperpolarizing photoreceptors of the scallop. Effects of tetraethylammonium and 4-aminopyridine. *J. Gen. Physiol.* 104:487–505. https://doi.org/10.1085/jgp.104.3.487

Gomez, M.P., and E. Nasi. 1997a. Antagonists of the cGMP-gated conductance of vertebrate rods block the photocurrent in scallop ciliary photoreceptors. *J. Physiol.* 500:367–378. https://doi.org/10.1113/jphysiol.1997.sp022027

Gomez, M.P., and E. Nasi. 1997b. Light adaptation in *Pecten* hyperpolarizing photoreceptors. *J. Gen. Physiol.* 109:371–384. https://doi.org/10.1085/jgp.109.3.371

Gomez, M.P., and E. Nasi. 2000. Light transduction in invertebrate hyperpolarizing photoreceptors: Possible involvement of a G_o-regulated guanylate cyclase. *J. Neurosci.* 20:5254–5263.

Gomez, M., and E. Nasi. 2005. On the gating mechanisms of the light-dependent conductance in *Pecten* hyperpolarizing photoreceptors. *J. Gen. Physiol.* 125:455–464. https://doi.org/10.1085/jgp.200509269

Gomez, M.P., L. Espinosa, N. Ramirez, and E. Nasi. 2011. Arrestin in ciliary invertebrate photoreceptors: molecular identification and functional analysis *in vivo*. *J. Neurosci.* 31:1811–1819. https://doi.org/10.1523/JNEUROSCI.3320-10.2011

Gorman, A.L.F., and J.S. McReynolds. 1969. Hyperpolarizing and depolarizing receptor potentials in the scallop eye. *Science.* 165:309–310. https://doi.org/10.1126/science.165.3890.309

Gorman, A.L.F., and J.S. McReynolds. 1978. Ionic effects on the membrane potential of hyperpolarizing photoreceptors in scallop retina. *J. Physiol.* 275:345–355. https://doi.org/10.1113/jphysiol.1978.sp012193

Gotow, T., and T. Nishi. 2002. Light-dependent K^+ channels in the mollusc *Onchidium* simple photoreceptors are opened by cGMP. *J. Gen. Physiol.* 120:581–597. https://doi.org/10.1085/jgp.20028619

Gotow, T., and T. Nishi. 2007. Involvement of a Go-type G-protein coupled to guanylate cyclase in the phototransduction cGMP cascade of molluscan simple photoreceptors. *Brain Res.* 1144:42–51. https://doi.org/10.1016/j.brainres.2007.01.068

Hardie, R.C., and P. Raghu. 2001. Visual transduction in *Drosophila*. *Nature.* 413:186–193. https://doi.org/10.1038/35093002

Hestrin, S., and J.I. Korenbrot. 1990. Activation kinetics of retinal cones and rods: Response to intense flashes of light. *J. Neurosci.* 10:1967–1973.

Hillman, P., S. Hochstein, and B. Minke. 1983. Transduction in invertebrate photoreceptors: Role of pigment bistability. *Physiol. Rev.* 63:668–772. https://doi.org/10.1152/physrev.1983.63.2.668

Hodgkin, A.L., and P.M. Obryan. 1977. Internal recording of the early receptor potential in turtle cones. *J. Physiol.* 267:737–766. https://doi.org/10.1113/jphysiol.1977.sp011836

Jagla, B., N. Aulner, P.D. Kelly, D. Song, A. Volchuk, A. Zatorski, D. Shum, T. Mayer, D.A. De Angelis, O. Ouerfelli, et al. 2005. Sequence characteristics of functional siRNAs. *RNA*. 11:864–872. https://doi.org/10.1261/rna.7275905

Jiang, M., and N.S. Bajpayee. 2009. Molecular mechanisms of G_o signaling. *Neurosignals.* 17:23–41. https://doi.org/10.1159/000186688

Kojima, D., A. Terakita, T. Ishikawa, Y. Tsukahara, A. Maeda, and Y. Shichida. 1997. A novel G_o-mediated phototransduction cascade in scallop visual cells. *J. Biol. Chem.* 272:22979–22982. https://doi.org/10.1074/jbc.272.37.22979

Koyanagi, M., A. Terakita, K. Kubokawa, and Y. Shichida. 2002. Amphioxus homologs of G_o-coupled rhodopsin and peropsin having 11-*cis*- and all-*trans*-retinals as their chromophores. *FEBS Lett.* 531:525–528. https://doi.org/10.1016/S0014-5793(02)03616-5

Lisman, J.E., and Y. Sheline. 1976. Analysis of the rhodopsin cycle in limulus ventral photoreceptors using the early receptor potential. *J. Gen. Physiol.* 68:487–501. https://doi.org/10.1085/jgp.68.5.487

Luo, D.-G., T. Xue, and K.-W. Yau. 2008. How vision begins: An odyssey. *Proc. Natl. Acad. Sci. USA*. 105:9855–9862. https://doi.org/10.1073/pnas.0708405105

Makino, C.L., W.R. Taylor, and D.A. Baylor. 1991. Rapid charge movements and photosensitivity of visual pigments in salamander rods and cones. *J. Physiol.* 442:761–780. https://doi.org/10.1113/jphysiol.1991.sp018818

Matsuda, T., and C.L. Cepko. 2004. Electroporation and RNA interference in the rodent retina in vivo and in vitro. *Proc. Natl. Acad. Sci. USA*. 101:16–22. https://doi.org/10.1073/pnas.2235688100

McReynolds, J.S., and A.L.F. Gorman. 1970a. Photoreceptor potentials of opposite polarity in the eye of the scallop, *Pecten irradians*. *J. Gen. Physiol.* 56:376–391. https://doi.org/10.1085/jgp.56.3.376

McReynolds, J.S., and A.L.F. Gorman. 1970b. Membrane conductances and spectral sensitivities of *Pecten* photoreceptors. *J. Gen. Physiol.* 56:392–406. https://doi.org/10.1085/jgp.56.3.392

Miller, W.H. 1958. Derivatives of cilia in the distal sense cells of the retina of *Pecten*. *J. Biophys. Biochem. Cytol.* 4:227–228. https://doi.org/10.1083/jcb.4.2.227

Murray, A.R., S.J. Fliesler, and M.R. Al-Ubaidi. 2009. Rhodopsin: The functional significance of asn-linked glycosylation and other post-translational modifications. *Ophthalmic Genet.* 30:109–120. https://doi.org/10.1080/13816810902962405

Nasi, E., and M. del Pilar Gomez. 1999. Divalent cation interactions with light-dependent K channels. Kinetics of voltage-dependent block and requirement for an open pore. *J. Gen. Physiol.* 114:653–672. https://doi.org/10.1085/jgp.114.5.653

Nishi, T., and T. Gotow. 1998. Light-increased cGMP and K+ conductance in the hyperpolarizing receptor potential of *Onchidium* extra-ocular photoreceptors. *Brain Res.* 809:325–336. https://doi.org/10.1016/S0006-8993(98)00913-5

Pugh, E.N. Jr., and T.D. Lamb. 1993. Amplification and kinetics of the activation steps in phototransduction. *Biochim. Biophys. Acta.* 1141:111–149. https://doi.org/10.1016/0005-2728(93)90038-H

Reynolds, A., D. Leake, Q. Boese, S. Scaringe, W.S. Marshall, and A. Khvorova. 2004. Rational siRNA design for RNA interference. *Nat. Biotechnol.* 22:326–330. https://doi.org/10.1038/nbt936

Shichida, Y., and T. Yamashita. 2003. Diversity of visual pigments from the viewpoint of G protein activation: Comparison with other G protein-coupled receptors. *Photochem. Photobiol. Sci.* 2:1237–1246. https://doi.org/10.1039/B300434A

Shimamura, K., S. Hirano, A.P. McMahon, and M. Takeichi. 1994. Wnt-1-dependent regulation of local E-cadherin and alpha N-catenin expression in the embryonic mouse brain. *Development*. 120:2225–2234.

Su, C.Y., D.G. Luo, A. Terakita, Y. Shichida, H.W. Liao, M.A. Kazmi, T.P. Sakmar, and K.-W. Yau. 2006. Parietal-eye phototransduction components and their potential evolutionary implications. *Science.* 311:1617–1621. https://doi.org/10.1126/science.1123802

Terakita, A. 2005. The opsins. *Genome Biol.* 6:213. https://doi.org/10.1186/gb-2005-6-3-213

Terakita, A., T. Yamashita, N. Nimbari, D. Kojima, and Y. Shichida. 2002. Functional interaction between bovine rhodopsin and G protein transducin. *J. Biol. Chem.* 277:40–46. https://doi.org/10.1074/jbc.M104960200

Tokuyasu, K., and E. Yamada. 1959. The fine structure of the retina studied with the electron microscope. IV. Morphogenesis of outer segments of retinal rods. *J. Biophys. Biochem. Cytol.* 6:225–230. https://doi.org/10.1083/jcb.6.2.225

Trissl, H.W., A. Darszon, and M. Montal. 1977. Rhodopsin in model membranes: Charge displacements in interfacial layers. *Proc. Natl. Acad. Sci. USA*. 74:207–210. https://doi.org/10.1073/pnas.74.1.207